

Metrology Studies and Baseplate-Pixel Sensor Gluing of the Pixel Strip Modules for the CMS II Phase Upgrade

Author:

Jem Aizen M. GUHIT

Supervisors:

James KEAVENEY

Marino MISSIROLI

Abstract

The upcoming High-Luminosity (HL) upgrade to the Large Hadron Collider (LHC) has set in motion the Central Muon Solenoid (CMS) Phase II Upgrade on its silicon tracker. To withstand the problems the current tracker cannot solve, such as the increase in data rates, pile up, and radiation damage, a new module with two silicon sensors closely spaced in a sandwich configuration is capable of discriminating between high and low transverse momentum. This configuration allows the tracker to provide information in the first level trigger decision. In order to prolong the lifetime of the modules during operation, an efficient cooling system has to be embedded within the components. This report outlines the advances and improvement made on the gluing techniques between the baseplate and pixel sensor of the pixel strip (PS) modules. The techniques were tested and produced promising results. Also, another important studies made was on the alignment of the silicon sensors. Methods on Metrology were developed using the capabilities of the newly commissioned microscope in the Detector Assembly Facility (DAF) at DESY. A relative angular tilt was found between the XY Stage and the microscope, which was then analytically calculated and was used as a correction to the measured values. These measurements were compared to the previous SmartScope Data.

Table of Contents

1	Introduction	3
1.1	The Large Hadron Collider	3
1.2	HL - LHC	3
1.3	CMS Experiment	4
1.4	CMS Phase II Tracker Upgrade	4
1.5	Pixel Strip Module	5
1.5.1	Baseplate-Pixel Sensor Gluing	5
1.5.2	Metrology	6
2	Equipment and Software	6
3	Baseplate-Pixel Sensor Gluing	7
3.1	Previous Method	7
3.2	New Proposed Method	8
4	New Method Trials	9
4.1	Trial 1	9
4.1.1	Trial 1: Results and Observations	10
4.2	Trial 2	10
4.2.1	Trial 2: Results and Observations	12
4.3	Trial 3	13
4.3.1	Trial 3: Results and Observations	14
5	Metrology	15
5.1	Horizontal and Vertical Method	15
5.1.1	Results	16
5.2	Diagonal Method	16
5.2.1	Results	17
5.3	Problems and Calibration	17
5.4	Corrections	18
5.5	Misalignment Angles	22
5.5.1	Horizontal and Vertical Line Method	22
5.5.2	Diagonal Line Method	23
6	Conclusion	24
7	Next Steps	24

1 Introduction

1.1 The Large Hadron Collider

The Large Hadron Collider (LHC) is one of the worlds largest and powerful particle accelerator. The LHC can accelerate different particles ranging from protons and heavy ions, and has facilitated collisions such as protons (p-p), lead ions (Pb-Pb), and protons on lead ions (p-Pb). With the current capabilities of the LHC, the collision rate of p-p collisions increased steadily, with instantaneous luminosities of up to $2.1 \times 10^{32} \text{cm}^{-2} \text{s}^{-1}$ in 2010, continuing to $7.7 \times 10^{33} \text{cm}^{-2} \text{s}^{-1}$ in 2012, and finally to $1.5 \times 10^{34} \text{cm}^{-2} \text{s}^{-1}$ in 2016, which exceeded the LHC's initial design luminosity value of $1.0 \times 10^{34} \text{cm}^{-2} \text{s}^{-1}$. [1]

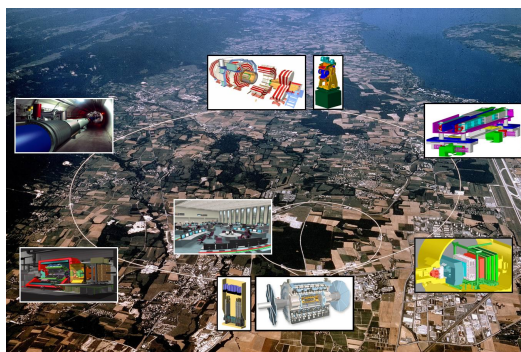


Figure 1: The Large Hadron Collider at CERN and its experiments [2]

1.2 HL - LHC

Due to the excellent performance of the LHC and its experiments, as shows in Figure 1, a proposal has been made and approved to upgrade the accelerator to instantaneous peak luminosities of $5 \times 10^{34} \text{cm}^{-2} \text{s}^{-1}$. The HL-LHC upgrade will greatly expand the physics potential of the LHC, in particular for rare and statistically limited standard model (SM) and beyond standard model (BSM) processes. Figure 2 shows LHC's timeline of runs, shutdowns, and scheduled upgrade.

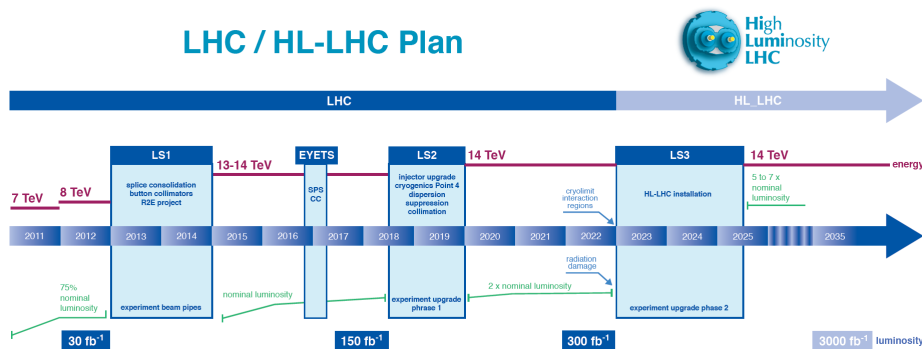


Figure 2: High-Luminosity LHC Timeline [3]

1.3 CMS Experiment

The Compact Muon Solenoid (CMS) Experiment is a general-purpose detector designed in the LHC to observe physics phenomena. CMS can be likened to a camera, which take photographs of particle collisions from all directions at a frequency of 40 MHz [4]. Even though particles produced in the primary collisions are unstable, they quickly transform into stable particles (photons, electrons, and hadrons) that can be detected. The identification of stable particles per collision, measurement of momenta and energy are needed to reconstruct the image of the collision.

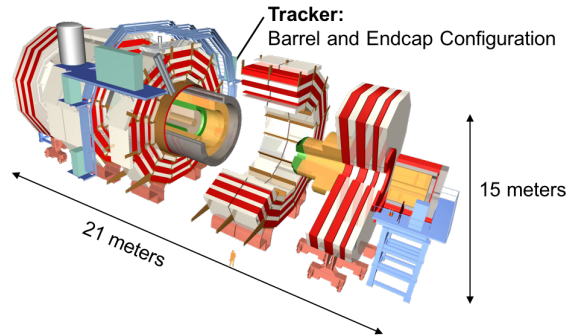


Figure 3: The CMS Detector and its dimensions [5]

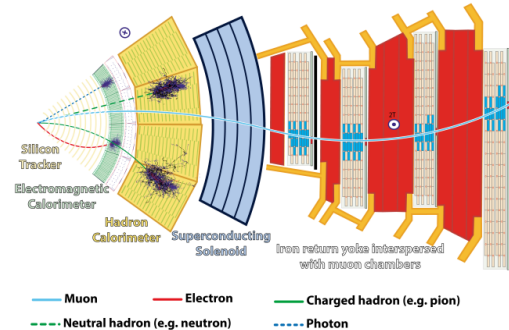


Figure 4: A Transverse Slice through the CMS Detector [6]

In Figure 3, it can be observed that the CMS detector is compact for the material it contains with dimensions 15 metres high and 21 metres long. It is also designed to detect muons accurately and consists of a large solenoid magnet with a magnetic field of 4 Tesla. On the other hand, Figure 4 shows a transverse slice of the detector which shows the individual components that have different purposes: Bending of Particles, Identifying Tracks, Measuring Energy, and Detecting Muons [4].

1.4 CMS Phase II Tracker Upgrade

Due to the increase in luminosity, the current tracker of the CMS would experience some problems:

- Increase in Data Rates: the current tracker cannot handle the increased event rates and readout of data
- Increase in Pile-Up: Occurs due to multiple interactions because of the increase in collisions
- Radiation Damage: the current tracker would deteriorate exponentially and cannot withstand the demands of high luminosity

Therefore, the upgrade needs a new tracker that can provide information for the first level trigger decision at the hardware level. The Pixel Strip (PS) Modules are currently being researched, commissioned, and prepared for the upcoming HL-LHC upgrade in 2024. [1]

1.5 Pixel Strip Module

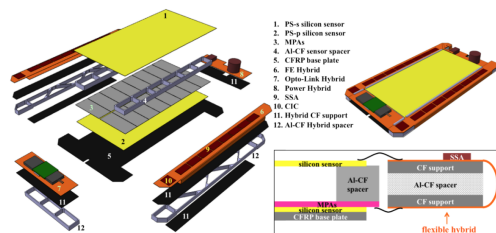


Figure 5: Exploded view of the Pixel Strip (PS) Module [7]

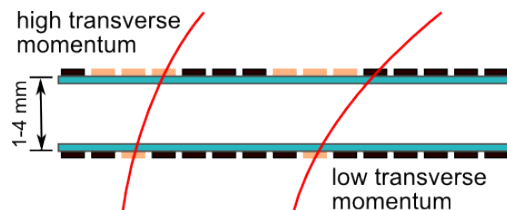


Figure 6: Triggering at Hardware Level [7]

The Pixel Strip (PS) Module is composed of two closely spaced silicon sensors in a sandwich configuration that allows the module to measure track momentum, as shown in Figure 5. It is designed with two silicon sensors on top of each other separated by a spacer and attached to readout electronics. This configuration can do tracking at a hardware level, as shown in Figure 6, the red lines called "stubs" represent the momentum of a particle. Due to the strong solenoid magnet of the CMS, the bending of particle is characterized by its momentum, high transverse momentum bend less than low transverse momentum particles. Hence, the PS Module can discriminate between high and low transverse momenta.

1.5.1 Baseplate-Pixel Sensor Gluing

To meet the demands of the high-luminosity upgrade, the PS Module must sustain a long lifetime. In order to prolong the operation of the modules, efficient cooling is crucial within the components. The basic idea is when an ionized particle hits the silicon detector, it disrupts the silicon's crystal lattice structure which produces electron-hole pairs. With the silicon sensor's built in applied voltage (band gap) and electric field, it produces a leakage current that hits either the pixel or strip electrode which are then known as readouts of the particle being detected. However, due to the silicon's crystal lattice structure, the bonds are only intact when the temperature is 0 Kelvin. However, that is not always the case. Therefore as the temperature increases, even there is no charged particle hitting the silicon sensors, there will be production of electron-hole pairs and will produce more leakage current at the electrodes. However, increase in leakage current generates more heat, which becomes a cycle shown in Figure 7.



Figure 7: Radiation damage on silicon sensors and relationship to cooling

The contact in between the cooling the component is mediated by a glue layer. Therefore, a gluing technique has to be developed in order to produce a good thermal contact between the components of the module. A good thermal contact can be characterized as a thin glue layer with minimal air bubbles, because thin layer increases the amount of dissipated heat and the presence of air bubbles inhibits cooling.

1.5.2 Metrology

Another important aspect of the PS Module is the alignment of the components. The Detector Assembly Facility (DAF) in DESY has commissioned a new microscope that can be used to measure the relative angular alignment between the two silicon sensors. The goal of the metrology study is to test the new microscope and compare the calculations from the SmartScope Machine (the machine previously used to measure the alignment of the sensors).

2 Equipment and Software

For the baseplate-pixel sensor gluing, an automated assembly has been commissioned for building the PS Modules. The hardware as shown in Figure 8 is operated by a developed computer software.

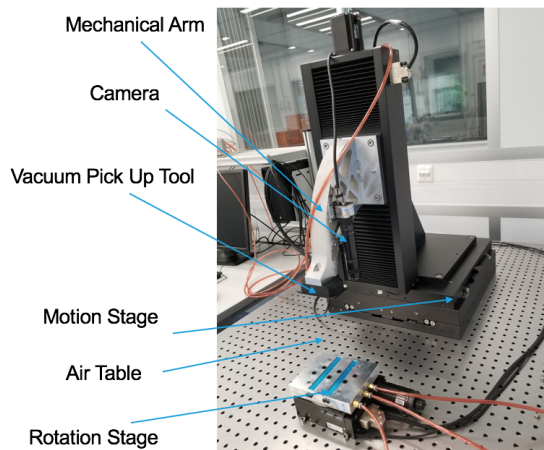


Figure 8: Automated Assembly Hardware Parts

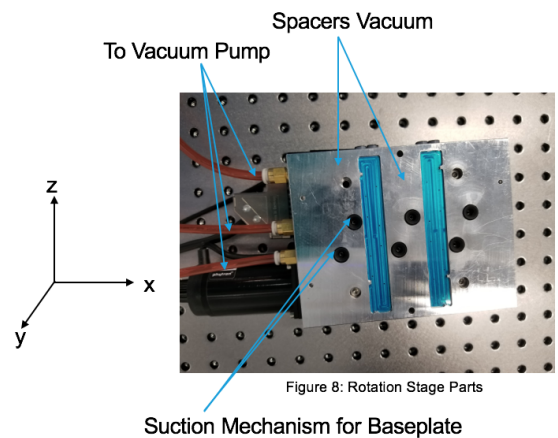


Figure 9: Rotational Stage Parts

Important parts that were used:

- Mechanical Arm: controls z-axis movements
- Vacuum Pick-Up Tool: attached to the mechanical arm that is responsible for holding the sensors
- Motion Stage: responsible for movements in the X and Y axis
- Air Table: suppress vibrations and other external movements
- Rotational Stage: responsible for holding the baseplate and also has its own vacuum system.

For the metrology studies, the microscope as shown in Figure 10 has the following features,

- Different lighting setups
- Measurement Schemes: In particular the XY Planar Measurements

- 200 - 200x Magnification
- HDR Imaging and Recording



Figure 10: New commissioned microscope for the metrology studies

The new microscope is beneficial for the PS Module Metrology because the large magnification range creates more precise measurements. Also, the edge detection option in the XY Planar Measurement automatically detects the corner of the reference object which increases the efficiency of measuring time.

3 Baseplate-Pixel Sensor Gluing

In order to utilize the capabilities of the automated assembly, two types of glues would be used: fast curing glue and slow curing glue. A small amount of fast curing glue is needed in order to ensure the parallelness between the components when being moved in the automated assembly. On the other hand, another glue must provide a strong adhesion over a wide range of temperatures and must withstand radiation. In order to facilitate the dissipation of heat the sensors generate during operation, the glue layer has to be thin, which can only be achieved by using low-viscosity slow curing glues.

3.1 Previous Method

The initial method tested for the commission of automated assembly for PS Modules.

1. The baseplate is placed onto the rotational stage with the vacuum pump on to keep it in place. Place the bottom sensor on top of the baseplate. Using the motion stage in the z-axis, pick up the sensor to a reasonable height.
2. To prepare the glue: Mix 7.5g Polytec LV 601 Part A and 2.5 Polytec LV 601 B with a 100:35 ratio in a weighing scale. Using the Fluid Mixer Machine input the following specifications:

- Mixing:
 - Time: 5 minutes
 - Rotational Speed: 900 revolutions per minute (rpm)
- Deforming:
 - Time: 4 minutes
 - Rotational Speed: 1200 rpm

Open the Fluid Mixer and remove the cup with the glue mixture and set aside.

3. From the cup, pour the slow curing glue to the baseplate and use a squeegee, a tool with a flat, smooth blade, to control the flow of the slow curing glue on the baseplate. Put a small amount of Loxeal and mix vigorously for 30 seconds, and using a needle apply to the corners of the baseplate.
4. Using the motion stage (z-axis), slowly bring the bottom sensor down to the baseplate for the components to bind. Do not move the set-up for 15 minutes to allow the fast curing glue to become inert. Then place the baseplate-pixel sensor in a curing area for 24 hours to allow curing of the slow curing glue.

Problems with the current method:

- Uneven layer of glue
- A large amount of air bubbles are formed

3.2 New Proposed Method

Based on the previous method, we developed a potential baseplate-pixel sensor gluing technique that aims to achieve the following specifications:

- Thin Layer of Glue
To facilitate dissipation of heat generated by the sensors during operation the layer of the glue has to be thin, which can be achieved using low viscosity type of glues.
- Minimal Air Bubbles
The presence of air bubbles inhibits cooling
- Integration of fast and slow glue It is important that there will be minimal reaction between the two type of glues

For the new proposed method, instead of silicon sensors we will be using glass sensors with the same dimensions in order to save resources. In addition, the Carbon Fiber Reinforced Polymer (CFRP) Base plate was the same material used in the original specifications for the PS Module.

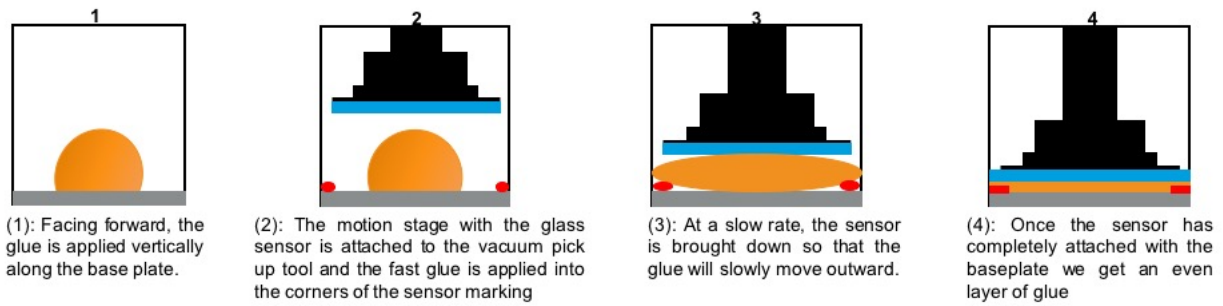


Figure 11: Potential method for the baseplate and pixel sensor gluing

4 New Method Trials

4.1 Trial 1

The goal of this trial is to observe the amount of air bubbles formed, so the amount of glue dispensed was done by eye.

1. To prepare the glue: Mix 7.5g Polytec LV 601 Part A and 2.5 Polytec LV 601 B with a 100:35 ratio in a weighing scale. Using the Fluid Mixer Machine input the following specifications:
 - Mixing:
 - Time: 5 minutes
 - Rotational Speed: 900 revolutions per minute (rpm)
 - Deforming:
 - Time: 4 minutes
 - Rotational Speed: 1200 rpm

After mixing transfer the glue mixture to a syringe and set aside until the baseplate is ready.

2. Using the rotational stage, put the baseplate and turn on the vacuum to hold it in a fix position. Position Bottom sensor on the baseplate followed by the vacuum pick up tool.
3. Using a non-permanent marker, trace the outline of the bottom sensor on the baseplate. Use the vacuum pick-up tool to move the bottom sensor up and away from the bottom sensor.
4. Using the syringe, slowly dispense glue vertically into the baseplate. Open the bottle of loxal and pour a small amount in a cup. Using a metallic stick, mix the glue vigorously for 30 seconds. Then apply the loxal into the corners of the baseplate.
5. Using the motion stage (z-axis) lower the bottom sensor using the vacuum pick-up tool in a slow rate until it completely sticks to the glue layer and baseplate. Leave the setup untouched for 10 minutes.

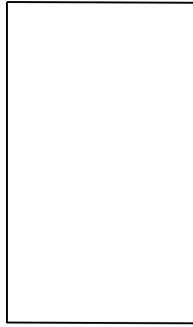


Figure 12: Outline of the marker for Trial 1

4.1.1 Trial 1: Results and Observations

After the 24-hour curing time, the slow curing glue went over the sides of the sensor, since the slow curing glue dispensed was done by eye. On the other hand, positioning the glue vertically in the baseplate and slowly moving outward after contact with the sensor produced minimal bubbles. From the trial, the next step would be to calculate the amount of glue with respect to the layer thickness. Also, outlining additional markers to the baseplate will improve the positioning of the fast and slow curing glues in order to give an excellent coverage without excess.

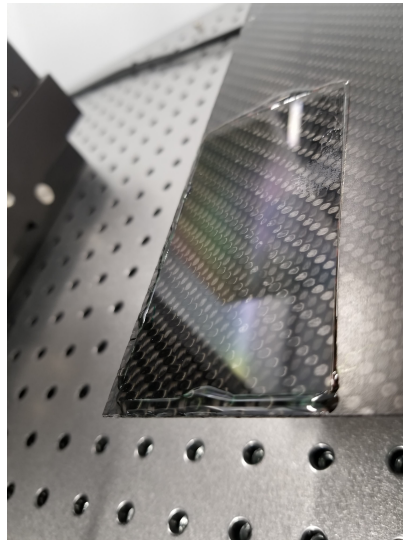


Figure 13: Baseplate and Sensor after 24-hour curing

4.2 Trial 2

In this trial the amount of glue dispensed was calculated. Using CMS Specifications, there are three potential slow curing glue layer thicknesses: $25 \mu\text{m}$, $50 \mu\text{m}$, and $75 \mu\text{m}$. Using the dimensions of the bottom pixel sensor with a length of 49mm and a height 98.5mm, the volume was calculated.

$$Volume = (length)(width)(height) \quad (1)$$

Using the specific gravity of the glue mixture: 1.15 g/cm^3 , we derived the mass of glue. For Trial 2, we chose option 2, 0.278g of slow curing glue.

$$V_1 = (49\text{mm})(98.5\text{mm})(0.025\text{mm}) = 120.66\text{mm}^3 \sim 0.139\text{g}$$

$$V_2 = (49\text{mm})(98.5\text{mm})(0.050\text{mm}) = 241.33\text{mm}^3 \sim 0.278\text{g}$$

$$V_3 = (49\text{mm})(98.5\text{mm})(0.075\text{mm}) = 361.99\text{mm}^3 \sim 0.416\text{g}$$



Figure 14: The baseplate was transferred from the rotational stage to the weighing scale to measure the amount of glue

1. To prepare the glue: Mix 7.5g Polytec LV 601 Part A and 2.5 Polytec LV 601 B with a 100:35 ratio in a weighing scale. Using the Fluid Mixer Machine input the following specifications:
 - Mixing:
 - Time: 5 minutes
 - Rotational Speed: 900 revolutions per minute (rpm)
 - Deforming:
 - Time: 4 minutes
 - Rotational Speed: 1200 rpm

After mixing transfer the glue mixture to a syringe and set aside until the baseplate is ready.

2. Using the rotational stage, put the baseplate and turn on the vacuum to hold it in a fix position. Position Bottom sensor on the baseplate followed by the vacuum pick up tool.
3. Using a non-permanent marker, trace the outline of the bottom sensor on the baseplate. Use the vacuum pick-up tool to move the bottom sensor up and away from the bottom sensor. Turn off the vacuum of the rotational stage to remove the baseplate.

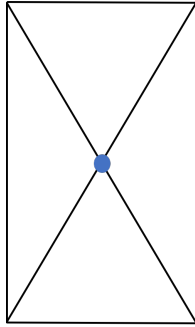


Figure 15: Outline of the marker for Trial 2

4. Transfer the baseplate to the weighing scale. Using the syringe, slowly dispense glue until the reading shows 0.278g. Transfer the baseplate back to the rotational stage. Using the vacuum pick-up tool, lower the bottom sensor slowly to re-align with the baseplate.
5. Open the bottle of loxal and pour a small amount in a cup. Using a metallic stick, mix the glue vigorously for 30 seconds. Then apply the loxal into the corners of the baseplate. Continue lowering the bottom sensor using the vacuum pick-up tool in a slow rate until it completely sticks to the glue layer and baseplate. Leave the setup untouched for 10 minutes.

4.2.1 Trial 2: Results and Observations

Similar to Trial 1, we observed that the slow curing glue leaked on one side of the sensor. Since after outlining the markers from Figure 5, the baseplate has to be moved to the weighing scale to measure the glue then was transported back. There is a possibility that the baseplate and sensor were not as parallel after applying the glue. Therefore, for the next trial our goal was to fix the alignment between sensor and baseplate after gluing and additional markers for the baseplate.

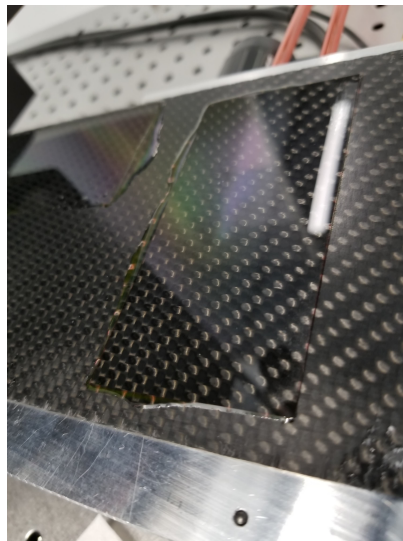


Figure 16: Baseplate and sensor after 24-hour curing

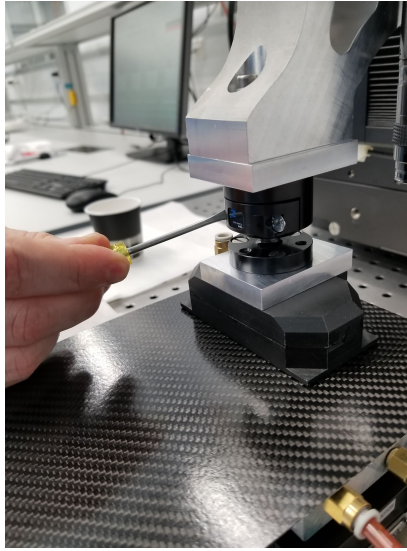


Figure 17: New experimental setup for the method including the ball joint on the motion stage. Calibrating the ball joint to be parallel to the baseplate

4.3 Trial 3

There are two improvements:

- **Ball Joint**
The tool is attached to the vacuum pick up tool and can be rotated. It can improve the parallelness between the baseplate and the sensor.
- **Additional Markers**
The position of the slow curing glue has to be equidistant from the center in order to achieve a symmetric glue layer.

Since we want to quantify the actual glue layer thickness, we measured the width of the baseplate and glass sensor without the glue layer, which was approximately $\sim 0.84\text{mm}$.

1. To prepare the glue: Mix 7.5g Polytec LV 601 Part A and 2.5 Polytec LV 601 B with a 100:35 ratio in a weighing scale. Using the Fluid Mixer Machine input the following specifications:
 - **Mixing:**
 - Time: 5 minutes
 - Rotational Speed: 900 revolutions per minute (rpm)
 - **Deforming:**
 - Time: 4 minutes
 - Rotational Speed: 1200 rpm

After mixing transfer the glue mixture to a syringe and set aside until the baseplate is ready.

2. Using the rotational stage, put the baseplate and turn on the vacuum to hold it in a fix position. Position Bottom sensor on the baseplate followed by the vacuum pick up tool.

- Using a non-permanent marker, trace the outline of the bottom sensor on the baseplate. Use the vacuum pick-up tool to move the bottom sensor up and away from the bottom sensor. Turn off the vacuum of the rotational stage to remove the baseplate.

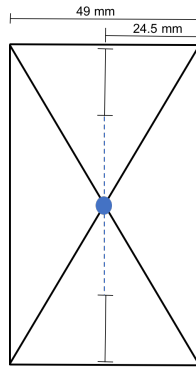


Figure 18: Outline of the marker for Trial 3

- Transfer the baseplate to the weighing scale. Using the syringe, slowly dispense glue until the reading shows 0.278g. Transfer the baseplate back to the rotational stage. Using the vacuum pick-up tool, lower the bottom sensor slowly to re-align with the baseplate.
- Open the bottle of loxal and pour a small amount in a cup. Using a metallic stick, mix the glue vigorously for 30 seconds. Then apply the loxal into the corners of the baseplate. Continue lowering the bottom sensor using the vacuum pick-up tool in a slow rate until it completely sticks to the glue layer and baseplate. Leave the setup untouched for 10 minutes.

4.3.1 Trial 3: Results and Observations

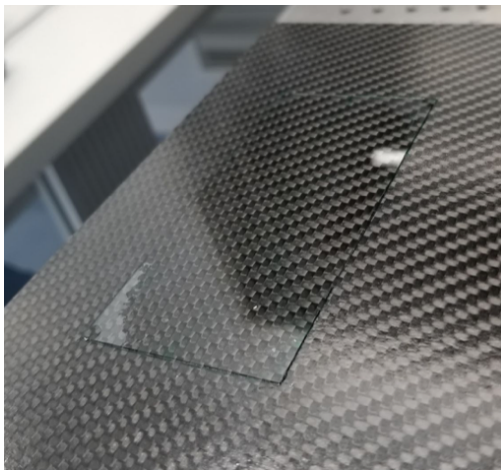


Figure 19: Baseplate and sensor after 5 minute fast glue curing time



Figure 20: Baseplate and sensor after 24-hour slow glue curing time

On Figure 9, it can be observed that there was an intentional gap between the fast glue and slow glue. This positioning between the glues allows the fast curing glue to become

inert. On the other hand, Figure 10 shows that through capillary action the slow curing glue filled the gap with minimal air bubbles. Furthermore, the thickness of the baseplate and the sensor with the glue layer was measured using a micrometer and was approximately between 0.84 - 0.85 mm.

5 Metrology

Another important aspect in the commissioning of the PS Modules is to ensure that it is working as expected. A quantifiable observable that can be used in order to check the module's capability is through the alignment of the sensors. In the previous construction of the dummy modules, measurements have been made using the SmartScope Measuring Tool in the previous laboratory. However, after moving to the new Detector Assembly Facility (DAF) Laboratory in DESY, a new type of microscope was brought and had to be tested whether it inputs similar results from the previous SmartScope measurements. Therefore, we developed two methods to check the alignment of the modules, the Horizontal and Vertical Line Method and the Diagonal Method.



Figure 21: New Microscope in the DAF Laboratory in DESY

5.1 Horizontal and Vertical Method

The Design Process

After choosing a fixed starting point, the microscope was used to measure the horizontal and vertical lines of the top and bottom sensors. The goal of this method is test the parallelness of the lines, given that this statement is true, the angle between the horizontal lines between bottom and top sensors must be zero degrees. Same follows with the vertical lines. A disadvantage in the method is that horizontal and vertical lines are not the longest line that can be measured in the module, therefore the angle is not fully constrained. Figure 12 shows the fixed point in the marker.

As shown in Figure 13, the solid lines represent the ideal horizontal and vertical lines that are aligned. However, there is a possibility, which is shown by the edged lines, of a

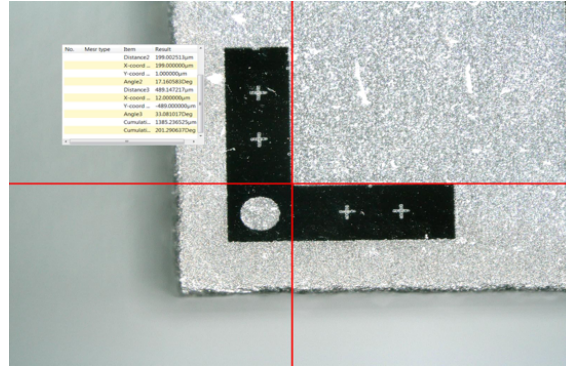


Figure 22: Each corner of the sensor has a marker and the image taken from the microscope shows the fixed point that will be used to measure the lines in all markers in the sensors

misalignment angle between the lines. Using the measurements, we can calculate for the angles of the horizontal lines of bottom and top sensor and calculate the delta theta between the lines, and same goes for the vertical lines.

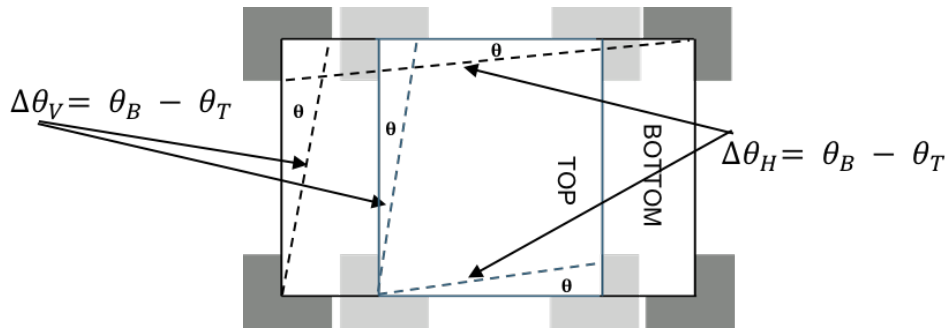


Figure 23: Metrology Misalignment Definition for Horizontal and Vertical Lines

5.1.1 Results

Given that the horizontal and vertical lines are aligned, the angle between the lines should be approximately 0 degrees or within tolerance. However, the resulting angles do not agree with the previous SmartScope Measurements.

5.2 Diagonal Method

The Design Process

Similar to the Horizontal and Vertical Method, the fixed point in Figure 12 was also used to measure the diagonal lines for both bottom and top sensor. The goal of the method is to measure the angle between the diagonals and subtract this value to the angle of the diagonals from the official values of the module. An advantage of the method is that diagonals are the longest lines that can be measured in the module, which constrains the misalignment angle. The definition of the diagonals is shown in Figure 24.

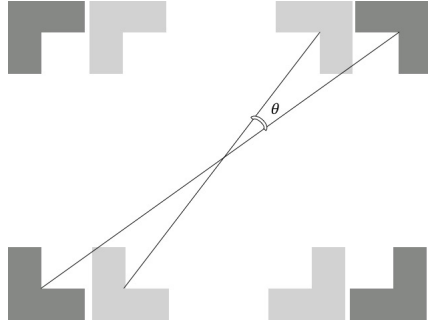


Figure 24: Metrology Misalignment Definition for Diagonal Lines

5.2.1 Results

Similar to the Horizontal and Vertical Line Method, the resulting misalignment angles do not agree with the previous SmartScope Measurements

5.3 Problems and Calibration

After finding out that the results from both methods were not consistent and disagreed with the previous measurements. We checked the measurements from the official CAD Drawings of the PS Module to determine whether the measurements from the microscope produce values that are within tolerance. We developed a calibration method by measuring the sides of the markers using the microscope. Afterwards, we calculated for the distances of each line and compared these values to the official CAD values of the PS Module.

Calibration by Markers

We observed that after comparing the experimental and official values, the shorter edge of the PS Module, 47 mm, have the largest deviation when the module's orientation was in a vertical direction. Also, experimental measurements were mostly smaller than the official values which led us to deduce that there might be a relative tilt between the stage and the microscope. Therefore, we took new measurements when the module's orientation was horizontal. Figures 25 and 26 shows the schematic of the marker calibration and the orientations consequently.

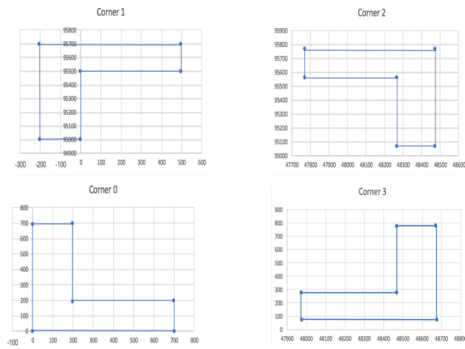


Figure 25: Schematic used to measure the sides of the markers

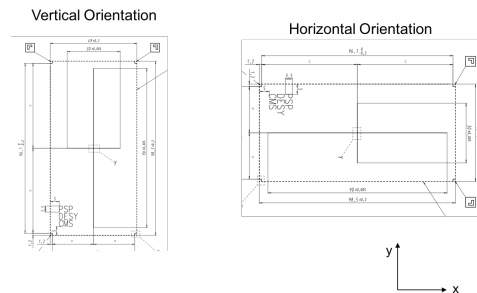


Figure 26: Horizontal and Vertical Orientations

If there is an evidence of a tilt, it should be the same for both bottom and top sensors. Hence, measurements were only taken for the top sensor. Based from the calculations, we found out that in the vertical orientation, the short edge (47 mm) has a larger deviation of 20 - 30 microns. While the long edge (95.7 mm) has a deviation of 5 - 20 microns with the deviation tolerance of ~ 5 microns. On the other hand, when the PS Module is in the horizontal orientation, the short edge (47 mm) has a deviation of only 0.5 - 8 microns. While the long edge (95.7 mm) has a deviation of 45 - 60 microns. The deviation of the short and long edge differs based on the orientation, which results from the relative tilt between the stage and microscope. Figure 27 and 28 shows the distances measured from the microscope for both vertical and horizontal orientation.

Vertical Orientation

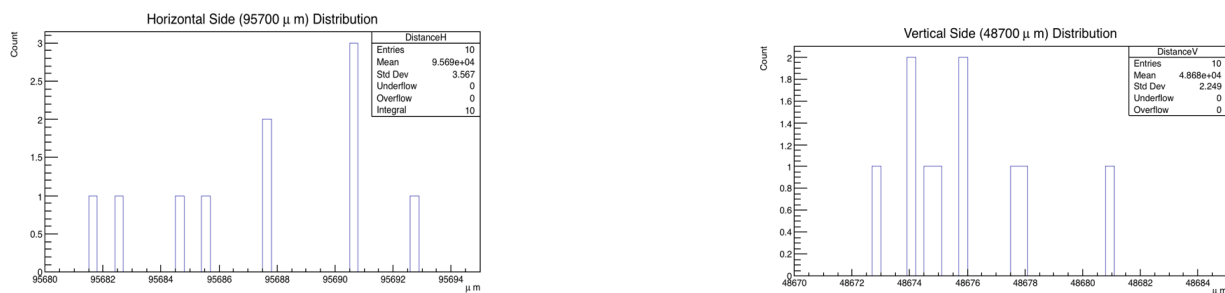


Figure 27: Distances of the long and short side for vertical orientation

Horizontal Orientation

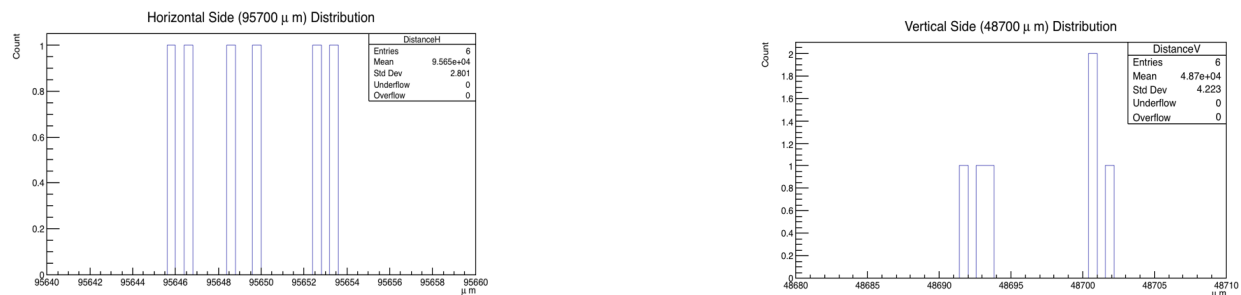


Figure 28: Distances of the long and short side for horizontal orientation

5.4 Corrections

After confirming the presence of a relative tilt between the X-Y stage and microscope, there were two possible options: calibrate the microscope or calculate for the tilt angle. Due to the availability of tools and circumstances, we couldn't calibrate the microscope during the duration of the summer program since we had to contact the company who sold the microscope. Therefore, we decided to calculate for the relative tilt in the X and Y axis.

Idea

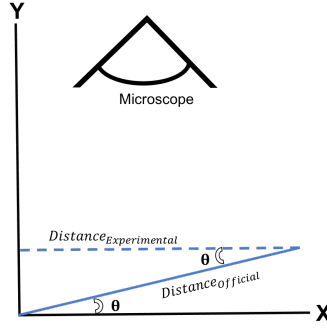


Figure 29: Geometry analysis behind the relative tilt

In Figure 29, the microscope is looking down at the X-Y Stage, where the θ is defined as the tilt. Therefore, the dashed lines are the values the microscope recorded, $Distance_{Experimental}$. Solving for θ would correct the previous values recorded and hence fix the misalignment angle values that we calculated. For this calculation, we used experimental coordinates measured from the microscope for the diagonals of both bottom and top sensor. The mean was calculated for the vertical and horizontal lines for the top and bottom sensors. This value was used to calculate for the tilt angle.

Method in Calculating Relative Tilt

$$\theta = \arccos \frac{Mean^*}{Distance_{official}} \quad (2)$$

* = there are four mean values:

- | | |
|--|---|
| <ul style="list-style-type: none"> • Top Sensor 1. Horizontal Lines 2. Vertical Lines | <ul style="list-style-type: none"> • Bottom Sensor 1. Horizontal Lines 2. Vertical Lines |
|--|---|

Afterwards, the mean value of theta was calculated for both horizontal and vertical lines so there are two relative tilt angle for the X and Y axis. Using the distance formula,

$$D = \sqrt{(X_{n+1} - X_n)^2 + (Y_{n+1} - Y_n)^2} \quad (3)$$

The corrected distances can be solved using the following formula:

$$Corrected_{Distance} = \frac{Distance_{experimental}}{\cos(\theta)} \quad (4)$$

The next step is to use the distance to transform the experimental coordinates to the corrected points in order to calculate the new misalignment angles. Translating of coordinates was done using the distance formula.

$$D_{new} = \sqrt{((X_{n+1} - X_{correction}) - X_n)^2 + ((Y_{n+1} - Y_{correction}) - Y_n)^2} \quad (5)$$

Example Calculation (Bottom Sensor only)

1. Point 1:

Original Coordinates: (0,0) and (-97.751, 0.777)

Original Distance: 97.754088

New Distance: 97.803236

$$\sqrt{[(-97.751 - A) - (0)]^2 + [(0.777 - A) - (0)]^2} = 97.803236$$

- squaring both sides -

$$(-97.751 - A)^2 + (0.777 - A)^2 = 9565.4729$$

- using system of equations -

$$A_1 \sim 0.0495305 \text{ and } A_2 \sim -97.0235$$

Using A_1 , Point 1: **(-97.8005305, 0.7274695)**

2. Point 2:

Original Coordinates: (-98.1200027, -47.5229988)

Original Distance: 48.301408

New Distance: 48.308457

Using the translated coordinate from Point 1,

$$\sqrt{[(-97.8005305) - (-98.1200027 - A)]^2 + [(0.7274695) - (-47.5229988 - A)]^2} = 48.308457$$

- squaring both sides -

$$(0.3194722 + A)^2 + (48.250468 + A)^2 = 2333.7070177208$$

- using system of equations -

$$A_1 \sim 0.0565254 \text{ and } A_2 \sim -48.6265$$

Using A_1 , Point 2: **(-98.1765281, -47.5795242)**

3. Point 3:

Original Coordinates: (-0.379999995, -48.2830009)

Original Distance: 97.742957

New Distance: 97.7921

Using the translated coordinate from Point 2,

$$\sqrt{[(-98.1765281) - (-0.379999995 - A)]^2 + [(-47.5795242) - (-48.2830009 - A)]^2} = 97.7921$$

- squaring both sides -

$$(-97.796528105 + A)^2 + (0.7034767 + A)^2 = 9563.29482241$$

- using system of equations -

$$A_1 \sim 0.007009073687 \text{ and } A_2 \sim 97.086042235$$

Using A_1 , Point 3: **(-0.3870090686, -48.29000997)**

Using the same method for the top sensor, the corrected coordinates are:

Bottom Sensor

- (0,0)
- (-97.8005305, 0.7274695)
- (-98.1765281, -47.5795242)
- (-0.3870090686, -48.29000997)

Top Sensor

- (-1.2430003, 0.0080000038)
- (-96.5422915645, 0.7617117375)
- (-96.9442816468, -47.5582801468)
- (-1.645000021, -48.2999993121)

Therefore, Figure 30 and 31 shows the differential mean of the uncorrected versus the corrected distances of the top sensor.

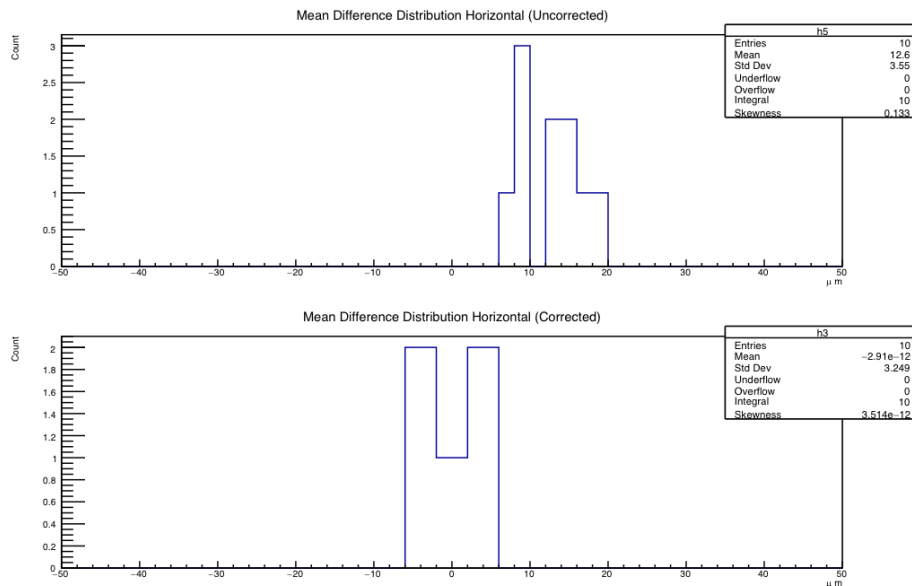


Figure 30: Mean Difference distribution between reference distance of the official CAD Drawing of the PS Module and the experimental values of the long side. The top plot shows the distribution for uncorrected values and bottom plot for the corrected values

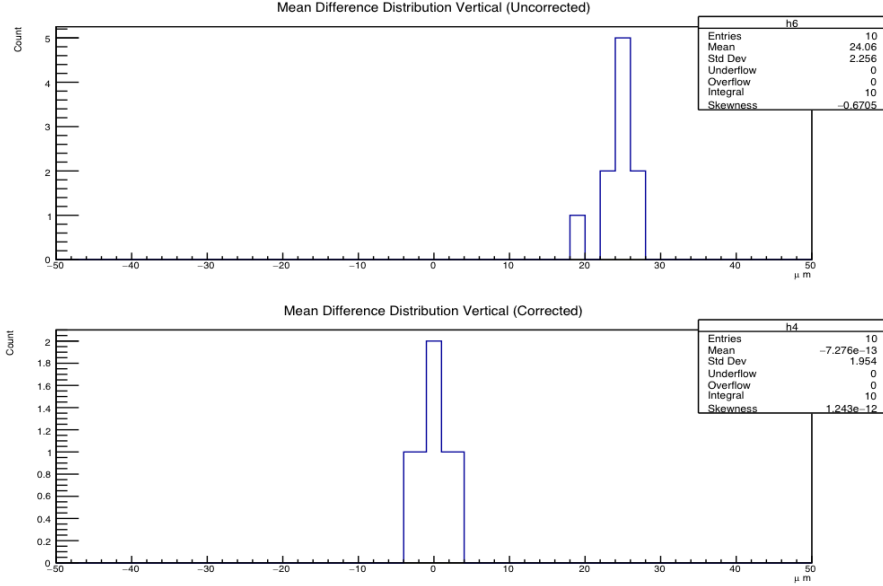


Figure 31: Mean Difference distribution between reference distance of the official CAD Drawing of the PS Module and the experimental values of the short side. The top plot shows the distribution for uncorrected values and bottom plot for the corrected values

5.5 Misalignment Angles

Using the corrected coordinates, the misalignment angles can be calculated.

5.5.1 Horizontal and Vertical Line Method

Horizontal Lines (95.7 mm)

- Solve for the slope of the horizontal lines for the top (m_1) and bottom sensor (m_2)
- To find the angle, use the equation $\theta = \arctan(m_n)$
- Find the difference in angle by subtracting the angle of the horizontal line of the bottom sensor with the angle of the horizontal line of the top sensor

$$\Delta\theta = \theta_1 - \theta_2 \quad (6)$$

- Since in the official CAD Drawing of the PS Module the values are precise, the $\Delta\theta$ of the horizontal lines are 0 radian, therefore the $\Delta\theta$ in equation 6 is the misalignment angle.

Vertical Lines (48.7 mm)

- Solve for the slope of the vertical lines for the top (m_1) and bottom sensor (m_2)
- To find the angle, use the equation $\theta = \arctan(m_n)$
- Find the difference in angle by subtracting the angle of the vertical line of the bottom sensor with the angle of the vertical line of the top sensor, use equation 6.

- Since in the official CAD Drawing of the PS Module the values are precise, the $\Delta\theta$ of the vertical lines are 0 radian, therefore the $\Delta\theta$ in equation 6 is the misalignment angle.

	Experimental Values	SmartScope Values
Long Side (95.7 mm)		
Side 1	470.5655	358.0995
Side 2	517.5623	420.2157
Short Side (48.7 mm)		
Side 1	535.7955	392.6575
Side 2	307.3148	421.3904

Table 1: Misalignment angles of corrected experimental and SmartScope measurements using Horizontal and Vertical Line Method

Table 1 shows the misalignment angle between the corrected experimental values and the re-calculated SmartScope values. To cross check whether the code used to calculate for the angles and the method of correction to the original coordinates worked, the misalignment of the SmartScope Values were calculated using the same code. Since the previous and the re-calculated SmartScope values matched, we gained confidence in the method and the code.

5.5.2 Diagonal Line Method

- Solve for the slope of the diagonal lines of the bottom and top sensor of the official CAD of the PS Modules and experimental corrected values
- Find the angles of the diagonal lines for the official and experimental values using $\theta = \arctan(m_n)$
- Using equation 6, find the delta theta of the official CAD values and the experimental values
- Since there is a residual angle from the official CAD measurements, subtract this value to the delta theta of the experimental values.

Residual Angle (from official CAD) = 0.01036 rad or \sim 0.5937 degrees

	Experimental Values	SmartScope Values
Diagonals		
Side 1	371.9489	463.5208
Side 2	595.6976	443.2887

Table 2: Misalignment angles of corrected experimental and SmartScope from the Diagonal Method

Since the residual angle of the diagonals from the official CAD drawing matched previous measurements. We have gained confidence that the misalignment angles measured in Figure 2 are consistent.

6 Conclusion

Baseplate-Pixel Sensor Gluing

After testing three important trials, the new proposed gluing technique for the baseplate and pixel sensor is promising but still needs fine tuning. From the tests, we have achieved our main goals: thin glue layer, minimal air bubbles, and good integration between fast and slow curing glue. The thin glue layer was achieved using the motion stage system. From Trial 3, the thickness of the baseplate and sensor with the glue layer was between 0.84 - 0.85 mm, which meant that the glue layer is in the order of 10 μm , which is better than the initial specifications. Consequently, minimal air bubbles were formed through the good positioning of fast and slow curing glue. This positioning improved because of detailed markers on the baseplate. Furthermore, there was a good integration of fast and slow curing glues. Visually there was no reaction between the glues. Also, the intentional gap between fast and slow curing glue was observed after contact in Figure 9, and through capillary action the slow curing glue filled the gap in Figure 10. From the trials, the current optimum slow curing glue amount is between 0.138 - 0.15g

Metrology

Based on the initial measurements, there was a relative tilt between the X-Y stage and the microscope which made the calculations not agree with the previous SmartScope data. Instead of fixing the tilt on the microscope, previous data was used to calculate for the tilt in the X and Y axis. The tilt angle corrected the distances and was used to translate the original points to the corrected coordinates. The previous SmartScope raw data was also analyzed using the same code developed over the duration of the summer program to compare whether the values are consistent with the previous measurements. The results of the two methods were consistent with the SmartScope data and there was confidence in the results of the experimental values.

7 Next Steps

For the baseplate-pixel sensor gluing, there is still an opportunity to further fine tune the amount of slow curing glue. Also the CMS Group at DESY is currently commissioning a Glue Machine that can automate the dispense of glue.

For the metrology, Using previous SmartScope Data to cross check current calculations, the microscope measurements agree with the SmartScope measurements between 100 - 150 microns. In the future, it is also possible to calibrate the relative tilt within the microscope instead of calculating the tilt angle.

References

- [1] CERN. The Phase 2 Upgrade of the CMS Tracker. *CMS Collaboration*, 17(001):13–17, 2017.
- [2] CERN. Lhc and experiments.
- [3] Antonella Del Rosso. Hl-lhc updates in japan.
- [4] CERN. Cms detector.
- [5] International Particle Physics Outreach Group. Cms detector.
- [6] CMS Collaboration. Cms detector slice.
- [7] James Keaveney. Commissioning of an automated assembly system for the PS modules of the CMS phase II upgrade outer tracker.. *Journal*, 11(1):1–5, 2013.